19th IFAC Symposium on Automatic Control in Aerospace
September 2-6, 2013. Würzburg, Germany

Path Generation and Control for Unmanned Multirotor Vehicles Using Nonlinear Dynamic Inversion and Pseudo Control Hedging

Thomas Raffler*, Jian Wang, Florian Holzapfel*****

** Institute of Flight System Dynamics, Technische Universität München, Germany, (e-mail: thomas.raffler@tum.de)*
*** Institute of Flight System Dynamics, Technische Universität München, Germany, (e-mail: jian.wang@tum.de)*
**** Institute of Flight System Dynamics, Technische Universität München, Germany, (e-mail: florian.holzapfel@tum.de)*

Abstract: This paper presents a new structure for path following control that allows multirotor UAVs to fly on predefined paths with high velocity. In contrast to pure trajectory tracking, it prioritizes spatial over temporal errors in case of actuator saturation. Path generation is achieved by a unit quaternion curve and an associated parallel transport frame in an interactive process, which leads to feasible paths of class C^3. The suggested control approach is composed of a nonlinear dynamic inversion trajectory controller and a path-based reference model with in-flight adjustable path velocity. By adopting the concept of pseudo control hedging, the tangential path progression is slowed down to the physically reachable velocity. Yaw rotation remains as an additional degree of freedom. Experimental flight tests are performed on a quadrotor with GPS receiver and low cost inertial sensors for state estimation. They demonstrate high velocity path following in the presence of thrust saturation, external disturbances and modeling uncertainties.

Keywords: Multirotor, Flight control, Path control, Trajectory planning, Feedback linearization, Pseudo control hedging

1. INTRODUCTION

The concept of fixed-pitch multirotor UAVs received remarkable attention from various research groups, hobbyists and companies due to its mechanical simplicity and robustness. By this time, a tremendous variety of linear and nonlinear control designs was presented in literature. Publications focussing on the position tracking problem already showed highly accurate and mature tracking performance.

Flight tests of trajectory controllers as presented in Valenti et al. (2006) and Bouabdallah et al. (2007) were conducted in a controlled lab environment and with feasible, low velocity trajectories where linear properties dominate. With the STARMAC program, Hoffmann et al. (2008) already showed successful outdoor flights with real-time trajectory planning and a velocity of up to 2 m/s. In Mellinger (2010) the authors present unprecedented three dimensional and high dynamic manoeuvres that show the physical capabilities of quadrotors. However, these results were obtained in a controlled lab environment with almost perfect measurements delivered by high speed, external motion capturing systems. Furthermore, there is no general solution to achieve this level of performance, but several distinct controllers for the different manoeuvres were implemented.

In order to allow dynamic and fast trajectories without too conservative velocity profiles, path following is investigated in this paper. This is especially useful for all applications where spatial control errors are more critical than temporal deviation. Examples for such applications are the navigation in constrained environments with obstacles or the movement of a flying camera along a predefined path. Compared to the tracking problem, path following received less attention but it is actively used for ground and marine vehicles. Although initial approaches had only local convergence and singularities for overlapping paths, Soetanto et al. (2003) were able to overcome these limitations by introducing a virtual target to define the current position on the desired path. Kaminer et al. (2010) applied this concept to a fixed wing UAV in SO(3) with an underlying commercial autopilot. Lately, Cichella et al. (2012) presented a Lyapunov based path following control for quadrotors with a focus on time synchronization. Relying on an external motion capturing system and the AR Drones attitude control, it is limited to comparably slow indoor manoeuvring.

This paper introduces a new path following concept applied to a nonlinear dynamic inversion controller for multirotor UAVs and is organized as follows. First, the construction of arbitrary feasible paths of class C^3 and the derivation of its kinematics are shown. Second, a control structure based on nonlinear dynamic inversion and pseudo control hedging is suggested, that uses the predefined path as a nonlinear reference model. After presenting the results of flight tests in numerical simulation, the paper concludes with outdoor test flights.

2. PATH GENERATION AND KINEMATICS

2.1 Notations and Definitions

Let there be a geometric curve $\vec{r}(l) \in \mathbb{R}^3$ which is regular and parameterized by arclength l. The class C^3 describes it as a function which is continously differentiable up to its third derivative. Time derivatives of e.g. $x(t)$ are denoted by $\dot{x}, \ddot{x}, \dddot{x}$ whereas x', x'' denote the derivative with respect to the path parameter. The symbols for kinematic relations are extended to inform about its notation coordinate frame and the relative reference. In this manner, the symbol $(\vec{v}^F)_F^N$ stands for the velocity of Point F relative to the Frame N, denoted in the Frame F. Rotation matrices are figured as e.g. $\boldsymbol{R}_{NF}$ which defines a vector's passive rotation from Frame F to N. The unit quaternion which parameterizes the equivalent rotation is written as $\breve{q}_{NF}$ and the circle operator denotes a quaternion multiplication. Occasionally, abbreviations without kinematic information are used and declared beforehand, e.g. $(\vec{r}^{NF})_N = \vec{r}(l)$.

2.2 Coordinate Frames

There are three coordinate systems in use which are depicted in Fig. 1. The Frame N is assumed to be an inertial frame wherein the path is defined. The Frame B with its reference point R defines the body fixed coordinate frame of the multirotor. As common in flight mechanics, the x-axis points to the front, the z-axis points down and is perpendicular to the rotor plane, and the y-axis completes the right-handed Cartesian frame. Frame F is attached to a moving point on the path and requires further explanation. An obvious choice for a coordinate frame associated to the curve, would be the Frenet-Seret frame which is directly defined by the curvature. Whereas it is very intuitive, it is undefined for straight path elements and is in general not rotating in a continuous way. As formally proved by Bishop (1975), there are more options how to define a coordinate frame with its first basis vector parallel to the tangential vector of the path. A parallel transport frame with a more detailed description in Hanson (1995) is chosen here.

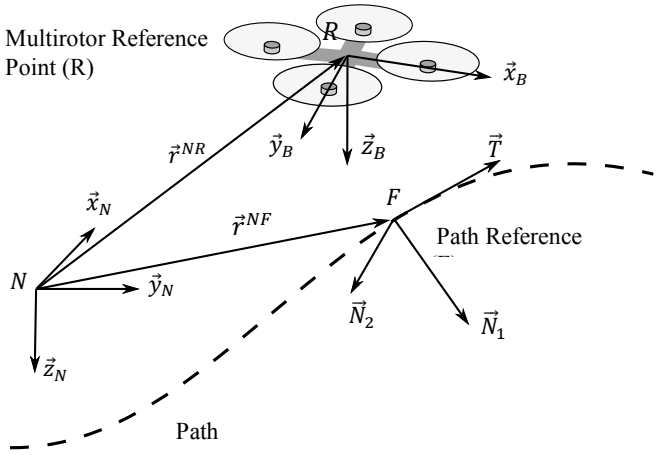

Fig. 1. Coordinate Frames.

In order to comply with previous publications, the parallel transport frame's basis vectors are written as.

$$\boldsymbol{R}_{NF} = \begin{bmatrix} \vec{T} & \vec{N}_1 & \vec{N}_2 \end{bmatrix}_N \tag{1}$$

with the path invariants k_1 and k_2 that define the curvature in $\vec{N}_1$ and $\vec{N}_2$, the Matrix derivative of (1) is given to

$$\frac{d\boldsymbol{R}_{NF}}{dl} = \begin{bmatrix} 0 & k_1 & k_2 \\ -k_1 & 0 & 0 \\ -k_2 & 0 & 0 \end{bmatrix} \begin{bmatrix} \vec{T} & \vec{N}_1 & \vec{N}_2 \end{bmatrix}_N \tag{2}$$

2.3 Path kinematics

For usage in the control design, the paths inertial derivatives are calculated in this section.

The velocity points along the tangential path vector and is parameterized with the path parameters derivative

$$(\vec{v}^F)_F^N = \begin{pmatrix} \dot{l} \\ 0 \\ 0 \end{pmatrix} \tag{3}$$

By the derivative of the associated parallel transport frame (2), the rotation of F w.r.t. N is given to

$$(\vec{\omega}^{NF})_F = \begin{bmatrix} 0 \\ -k_2 \\ k_1 \end{bmatrix} \dot{l} \tag{4}$$

The inertial acceleration of F can be calculated with an euler differentiation to

$$(\vec{a}^F)_F^{NN} = (\vec{a}^F)_F^{NF} + (\vec{\omega}^{NF})_F \times (\vec{v}^F)_F^N = \begin{pmatrix} \ddot{l} \\ k_1\, \dot{l}^2 \\ k_2\, \dot{l}^2 \end{pmatrix} \tag{5}$$

As the generated path is C^3, we can continue to derive the acceleration rate.

$$\begin{aligned} &\left(\dot{\vec{a}}^F\right)_F^{NNN} = \left(\dot{\vec{a}}^F\right)_F^{NNF} + (\vec{\omega}^{NF})_F \times (\vec{a}^F)_F^{NN} \\ &= \left(\dot{\vec{a}}^F\right)_F^{NFF} + \left(\dot{\vec{\omega}}^{NF}\right)_F \times (\vec{v}^F)_F^N + 2(\vec{\omega}^{NF})_F \times (\vec{a}^F)_F^{NF} \\ &+ (\vec{\omega}^{NF})_F \times [(\vec{\omega}^{NF})_F \times (\vec{v}^F)_F^N] \\ &= \begin{pmatrix} \dddot{l} - \dot{l}^3(k_1^2 + k_2^2) \\ \dot{k}_1\, \dot{l}^2 + 3\, k_1\, \dot{l}\, \ddot{l} \\ \dot{k}_2\, \dot{l}^2 + 3\, k_2\, \dot{l}\, \ddot{l} \end{pmatrix} \end{aligned} \tag{6}$$

The curvature time derivatives can be substituted by the derivative w.r.t. the path parameter.

$$\dot{k}_1 = k_1'\, \dot{l},\ \dot{k}_2 = k_2'\, \dot{l} \tag{7}$$

With (6) it follows the inertial acceleration rate of the path.

$$\left(\dot{\vec{a}}^F\right)_F^{NNN} = \begin{pmatrix} \dddot{l} - \dot{l}^3(k_1^2 + k_2^2) \\ k_1'\, \dot{l}^3 + 3k_1\, \dot{l}\, \ddot{l} \\ k_2'\, \dot{l}^3 + 3k_2\, \dot{l}\, \ddot{l} \end{pmatrix} \tag{8}$$

2.4 Path generation

As it is obviously possible to follow any arbitrary path with a multirotor configuration, the focus of path generation lies in paths that can be followed with high velocity and sufficient accuracy. The path to be generated defines the following path state vector for a parameter l.

$$\vec{x}(l) = [\vec{r} \quad \breve{q}_{NF} \quad k_1 \quad k_2 \quad k_1' \quad k_2']^T$$

According to (3), (5) and (8) this is sufficient to calculate all path derivatives as long as the path parameter and its derivatives are given. The path is generated as the special case of a unit quaternion integral curve similar to Miura (2000).

$$\vec{r}(l) = \vec{r}_0 + \int_0^l \breve{q}_{NF}(l) \circ \begin{pmatrix} 0 \\ 1 \\ 0 \\ 0 \end{pmatrix} \circ \breve{q}_{NF}(l) dl = \vec{r}_0 + \int_0^l \begin{pmatrix} \breve{q}_{NF,0}^2 + \breve{q}_{NF,1}^2 - \breve{q}_{NF,2}^2 - \breve{q}_{NF,3}^2 \\ 2\left(\breve{q}_{NF,1}\breve{q}_{NF,2} + \breve{q}_{NF,0}\breve{q}_{NF,3}\right) \\ 2\left(\breve{q}_{NF,1}\breve{q}_{NF,3} - \breve{q}_{NF,0}\breve{q}_{NF,2}\right) \end{pmatrix} dl \quad (9)$$

The path direction is the quaternion integral of the paths curvature with an arbitrary initial unit quaternion $\breve{q}_{NF}(0)$ that specifies the initial path tangent.

$$\breve{q}_{NF}(l) = \int_0^l \frac{1}{2} \cdot \breve{q}_{NF}(l) \circ \begin{pmatrix} 0 \\ 0 \\ -k_2 \\ k_1 \end{pmatrix} dl \quad (10)$$

The path integration is conducted in an interactive process which obeys one of the following constraints in order to ensure a sufficiently small path following deviation. If the desired velocity is the primary design objective, the curvature and its derivatives are constrained in order to respect the plants limits in acceleration and rotation rate. Or alternatively, a maximum design velocity is suggested which depends on the planned path curvature.

In order to get a path of class C^3 the desired curvature k_d is additionally filtered by a linear system of second order with critical damping and the natural frequency ω_p.

$$k''(l) + 2\omega_p k'(l) + \omega_p^2 k(l) = \omega_p^2 k_d(l) \quad (11)$$

As there exists a trivial analytical solution, the user inputs for path construction can be reduced to simple commands, e.g. 90 degree turn with specified normal vector and maximum curvature. With this approach it is possible to create a big variety of paths including straight lines, circular arcs and smoothed 3D clothoids. In the whole process, the desired maximal velocity is only a secondary information to estimate the control accuracy.

3. PATH CONTROL

*3.*1 *Nonlinear Dynamic Inversion Trajectory Control*

The underlying trajectory control follows the idea of Wang et al. (2011) and is described here only in short. The translational acceleration of a general multirotor system is mainly dependant of a normalized thrust input δ_T, the maximum achievable acceleration a_z, the attitude R_{NB}, velocity $\vec{v}_A$, and gravity $\vec{g}$. For the following control design it is assumed to be of following shape, where the function f describes the velocity dependant part of the propulsion forces.

$$(\vec{a}^R)_N^{NN} = \boldsymbol{R}_{NB} \begin{pmatrix} 0 \\ 0 \\ \delta_T\, a_z \end{pmatrix} + \vec{f}(\vec{v}_A) + \vec{g} \quad (12)$$

As only one control input appeared yet, δ_T is dynamically extended. With the euler differentiation rule, the acceleration rate is derived and the roll rate p as well as pitch rate q, show up.

$$\left(\dot{\vec{a}}^R\right)_N^{NNN} = \boldsymbol{R}_{NB} \begin{pmatrix} q\ \delta_T \\ -p\ \delta_T \\ \dot{\delta}_T \end{pmatrix} a_z + \frac{\mathrm{d}}{\mathrm{dt}} \vec{f}(\vec{v}_A) \quad (13)$$

Instead of a further dynamic extension, the rotation rates are considered as control inputs for a time scale separated inner loop. This is justified with the fast dynamics and the high control effectiveness of a multirotors rotation rate control. With the acceleration rate as virtual control input $\vec{\nu}$, Equation (13) can now be solved for p, q, and $\dot{\delta}_T$.

$$\begin{pmatrix} p \\ q \\ \dot{\delta}_T \end{pmatrix} = \frac{1}{\delta_T\, a_z} \begin{bmatrix} 0 & -1 & 0 \\ 1 & 0 & 0 \\ 0 & 0 & \delta_T \end{bmatrix} R_{BN} \left(\vec{\nu} - \frac{\mathrm{d}}{\mathrm{dt}} \vec{f}(\vec{v}_A) \right) \quad (14)$$

As it is physically not possible to command a negative or vanishing thrust, there is no critical singularity in the dynamic inversion.

Although the velocity dependant propulsion forces have a stabilizing effect on the translational dynamics, they can be cancelled for the following unidirectional relation, which is a conservative estimation of the real aerodynamic effects.

$$\vec{f}(\vec{v}_A) = -\, c_d\, \vec{v}_A \quad (15)$$

$$\frac{\mathrm{d}}{\mathrm{dt}} \vec{f}(\vec{v}_A) = -\, c_d \left(\boldsymbol{R}_{NB} \begin{pmatrix} 0 \\ 0 \\ \delta_T\, a_z \end{pmatrix} - \, c_d\, \vec{v}_A + \vec{g} \right) \quad (16)$$

A more detailed model is not desired in this context, as there is no direct measurement for the actual aerodynamic velocity available. An estimation of the wind vector is considered for future designs.

The yaw rate r has obviously no effect on translational motion and can thus be controlled at will.

In order to stabilize the translational error dynamics in the presence of modelling errors and disturbance, a linear error feedback is added to the pseudo control input.

$$\vec{\boldsymbol{\nu}} = \vec{\boldsymbol{\nu}}_{\boldsymbol{R}} + \boldsymbol{C_2}\ddot{\vec{\boldsymbol{e}}} + \boldsymbol{C_1}\dot{\vec{\boldsymbol{e}}} + \boldsymbol{C_0}\vec{\boldsymbol{e}} \quad (17)$$

The error dynamics are assigned by pole placement and under consideration of sensor data quality and time scale separation to the inner rate control loop.

3.2. Nonlinear Path Reference Model

Compared to a conventional trajectory tracking controller, the main modification is the nonlinear path reference model which is slowed down by pseudo control hedging. The reference model consists of two elements, a one-dimensional reference model for the path progression and a path state conversion which calculates the inertial reference trajectory.

The input of the former is the desired tangential path velocity which is adjusted in-flight by the UAV operator. It is filtered in a linear reference model of second order and integrated to obtain the path parameter l and its derivatives. While ω_v allows to define the dynamic response to user inputs, p_h is the pseudo control hedging input, which will be explained later.

$$\ddot{l} = \omega_v^2\left(\dot{l}_{des} - \dot{l}\right) - 2\omega_v\dot{l} - p_h \quad (18)$$

Together with the kinematic relationships (3), (5), (8) and the previously generated path parameterization $\vec{x}(l)$ it is now possible to calculate the pseudo control input ν_R as well as the reference signal ξ_R.

$$\vec{\xi}_R = [(\vec{r}^R)_N \quad (\vec{v}^F)_F^N \quad (\vec{a}^F)_F^{NN}]^T$$

Up to this point, it is already possible to adjust the velocity in-flight without modifying the desired path, but in terms of error dynamics it is still conventional trajectory tracking. In order to relax the temporal constraint, pseudo control hedging is introduced in the next section.

3.3 Pseudo Control Hedging

First suggested by Johnson et al. (2000), pseudo control hedging (PCH) proved to be an effective method to account for actuator dynamics in model reference adaptive control and nonlinear dynamic inversion. The idea is to hide the actuator dynamics from the error control by appropriately slowing down (hedging) the reference model. If applied to a conventional trajectory control, it would inadvertently modify the flight path in order to stay within the actuators capabilities. In the approach presented in this paper, only the path progression is slowed down, without modifying the reference path.

The reaction deficit in the path progression is the difference between commanded and estimated in-path acceleration. By comparing (8) and (13), the hedging signal can be given to

$$p_h = R_{FB,13}\left(\dot{\delta}_{T,cmd} - \dot{\delta}_{T,est}\right)a_z \quad (19)$$

Figure 2 shows the suggested structure with the nonlinear dynamic inversion trajectory control, the path reference model and an inner rate control loop.

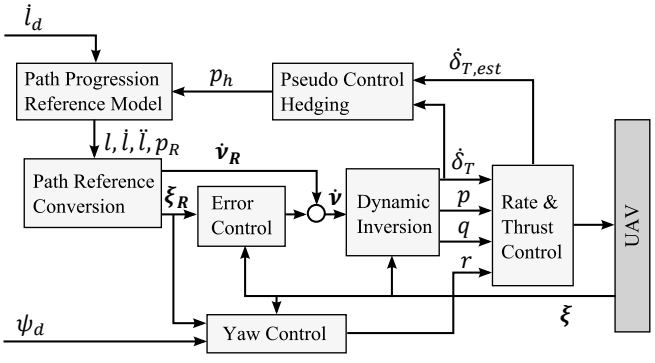

Fig. 2. Structural Overview.

3.4 Yaw Rate

The yaw rate is a remaining degree of freedom which does not influence the path control and thus can be controlled by application specific control modes. Besides a simple zero yaw rate law, it is e.g. possible to keep the x-axis in maximum alignment with the transport frame velocity vector. For the use case considered in this paper, the yaw rate is assumed to be governed by the onboard cameras discrete point-of-view control.

3.5 Rate & Thrust Control

In order to fulfil the time scale separation between inner and outer loop, the rate control has to be sufficiently fast and accurate. For the scope of this investigation, a simple linear PI error control is applied to the input-output linearized plant. The natural frequency of the error dynamics is set to 40 rad/s for roll and nick which gives sufficient time scale separation.

The squared mean motor RPM is assumed to be proportional to the overall thrust, but can have a big offset due to aerodynamic velocity. Thanks to the dynamic extension of thrust to $\dot{\delta}_T$, this approach is however less susceptible to constant uncertainties.

4. SIMULATION RESULTS

First, simulation results for the considered nominal plant are presented in order to support the theory. Figure 3 shows the desired path together with simulation results for the path reference trajectory controller with and without activated pseudo control hedging. Following parameters were used.

$$c_d = 2, \qquad 0.2 \le \delta_T \le 1, \qquad a_z = -22\ m/s^2$$

The simulation results clearly show the reference model being slowed down to a feasible velocity without altering the desired path. As expected, the controller without PCH behaves exactly like a trajectory controller that is not able to follow the reference model. Needless to say, there is no difference between both controllers as long as there is no actuator saturation.

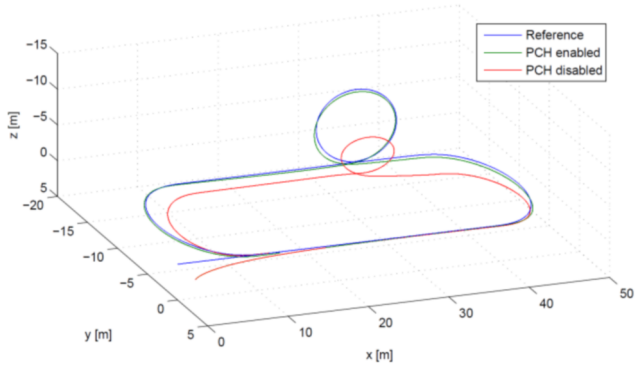

Fig. 3. Simulated flight paths with and without path PCH.

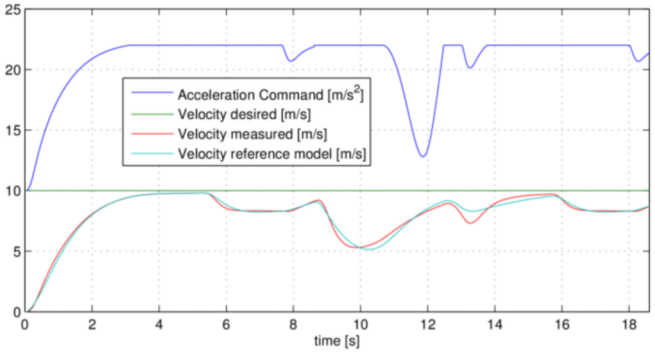

Fig. 4. Simulated flight velocity with enabled PCH.

5. EXPERIMENTAL VALIDATION

Before carrying out flight tests, the designed path controller is extensively tested in a high fidelity simulation environment. The FSD Multicopter Simulation Framework includes detailed models for aerodynamic forces, rigid body motion, actuator dynamics and inertial sensors. Real flight tests are then performed with an Asctec Hummingbird Quadrotor which is a successor of the system described in Gurdan et al. (2007).

In addition to the off-the-shelf UAV system, a Gumstix Computer-on-Module with custom flight control software framework is used to conveniently execute floating point algorithms generated with Matlab/Simulink.

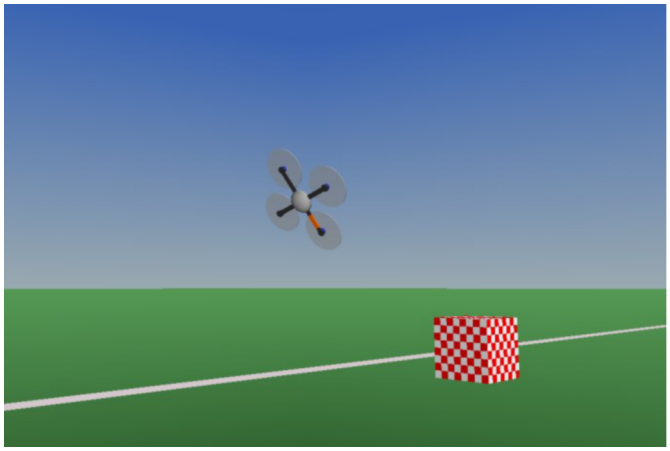

Fig. 5. Test flight with the FSD Multicopter Simulation

Fig. 6. Outdoor test flight with Asctec Hummingbird.

With a focus on robustness, comparably slow error dynamics were chosen for the preliminary test flights. In (17), one pole pair was set to the natural frequency of 1.7 rad/s and a damping of 0.7 and the real pole was set to 1.6 rad/s. The motor rpm was limited to the range [3000; 6000].

Despite varying wind speed and gusts of about 5 m/s the UAV still followed the previously simulated path. Note that the vertical loop which is part of the path can result in two different manoeuvres dependent on path velocity. For low speed, the path can be followed with ordinary attitude changes, whereas it has to do a full flip for high speed flight. Both trajectories are naturally possible by this approach and were successfully flight tested. Fig. 7 shows the first option which results in smaller path deviations.

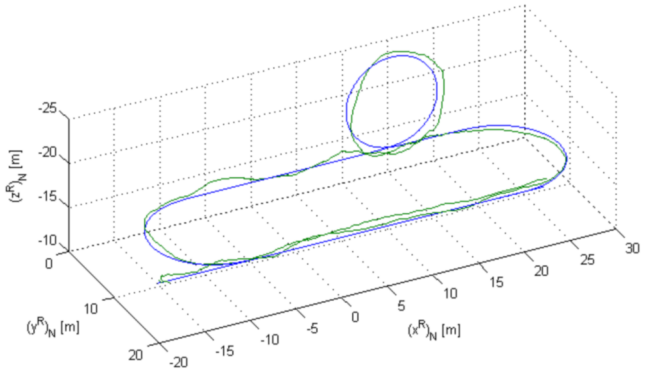

Fig. 7. Resulting test flight path for low velocity loop.

A second path was designed and flown with high velocities of up to 12 m/s as seen in Fig. 8 and Fig. 9. As the error dynamics remain the same, the resulting control errors due to uncertainties grow. While there are considerable control errors also in the velocity control, the concept of pseudo control hedging for a path based reference model proved its effectiveness. When it is physically not possible to reach the desired velocity, the path progression is slowed down appropriately as can be clearly seen in Fig. 9.

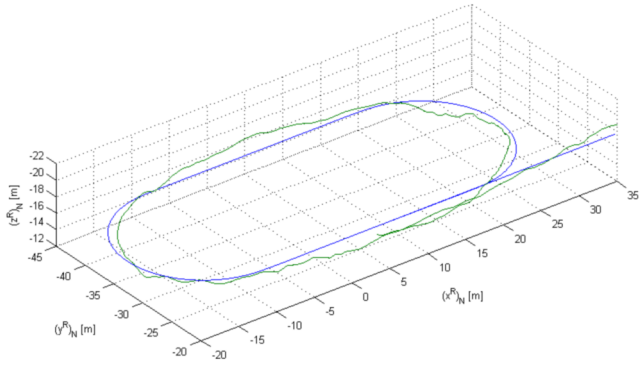

Fig. 8. Flat race track path flown with 12 m/s

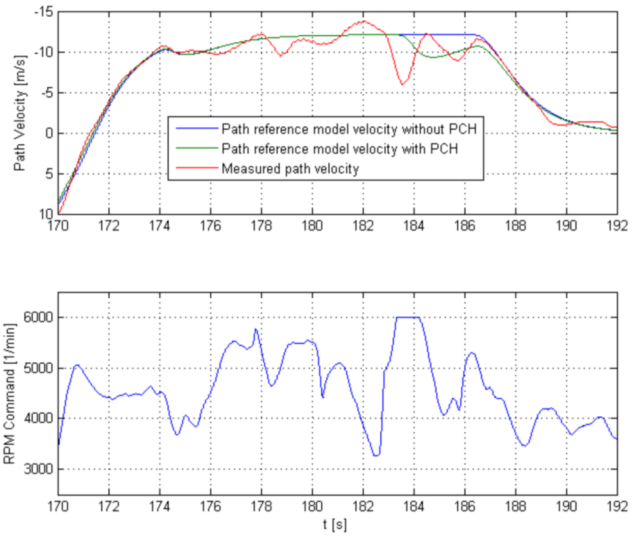

Fig. 9. Velocity and Motor RPM of race track path

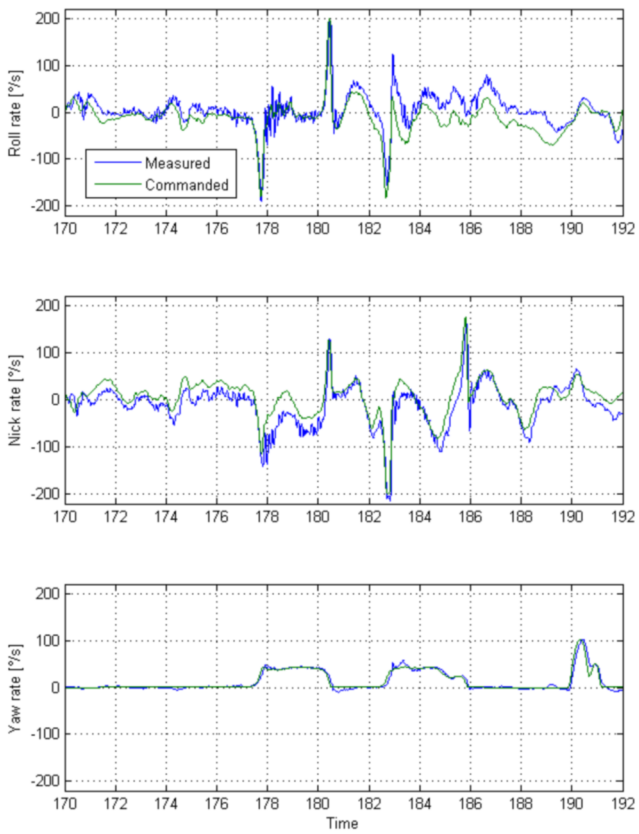

Fig. 10. Rate control tracking

5. CONCLUSIONS

The suggested approach for path following is straight-forward to implement in an existing system and bridges the gap between trajectory control and path control. For practical control applications it is already a valuable benefit to define the path a priori and to use the dynamically adjustable velocity for fulfilling secondary mission objectives. This can be especially useful for operators of a flying multirotor camera. Concerning high performance flight and robustness against external disturbance, the introduced path based reference model with pseudo control hedging provides an effective way to follow a given path in the presence of input saturation. Further research has to be done to improve the underlying trajectory controller by means of nonlinear error dynamics, more detailed aerodynamic models and adaptive control.

While it was applied here to a Multirotor UAV, this novel concept is suitable for a variety of other applications including helicopters, fixed-wing aircraft and ground vehicles.

ACKNOWLEDGEMENTS

The research of T. Raffler is supported by the German Federal Ministry of Economics and Technology.

REFERENCES

Bishop, R. (1975), There is More than One Way to Frame a Curve, *The American Mathematical Monthly*, Vol. 82, No. 3, pp. 246-251.

Bouabdallah, S., Siegwart, R. (2007), Full control of a quadrotor, Proceedings of the 2007 IEEE/RSJ International Conference on Intelligent Robots and Systems, pp. 153-158

Cichella, V., Kaminer, I., Xargay, E., Dobrokhodov, V., Hovakimyan, N., Aguiar, P., Pascoal, A. (2012), A Lyapunov-based approach for Time-Coordinated 3D Path-Following of Multiple Quadrotors, *51st IEEE Conference on Decision and Control*, Maui, USA.

Fritsch, O., De Monte, P., Buhl, M., Lohmann, B. (2012), Quasi-static Feedback Linearization for the Translational Dynamics of a Quadrotor Helicopter, *American Control Conference*, Montréal, Canada.

Gurdan, D., Stumpf, J., Achtelik, M., Doth, K.M., Hirzinger, G., Rus, D. (2007), Energy-efficient autonomous four-rotor flying robot controlled at 1 kHz, *Proceedings of the IEEE International Conference on Robotics and Automation (ICRA)*, pp. 361-366.

Hanson, A., Ma, H. (1995), Parallel Transport Approach to Curve Framing, *Department of Computer Science*, Indiana University, USA.

Hoffmann, G., Waslander, S., Tomlin, C. (2008). Quadrotor helicopter trajectory tracking control. *Proceedings of the AIAA Guidance, Navigation, and Control Conference*, Honolulu, Hawaii.

Johnson, E., Calise, A. (2000), Pseudo-Control Hedging: A New Method for Adaptive Control, *Advances in Navigation Guidance and Control Technology Workshop*, Alabama, USA.

Kaminer, I., Pascoal, A., Xargay, E., Hovakimyan, N., Cao, C., Dobrokhodov, V. (2010), Path Following for Unmanned Aerial Vehicles Using L1 Adaptive Augmentation of Commercial Autopilots, *Journal of Guidance, Control and Dynamics*, Vol. 33, No. 2, pp. 550-564.

Mellinger, D., Michael, N., Kumar, V. (2010), Trajectory generation and control for precise aggressive maneuvers with quadrotors, *Proceedings of the International Symposium on Experimental Robotics*, Delhi, India.

Miura, K. (2000), Unit quaternion integral curve: A new type of fair free-form curves, *Computer Aided Geometric Design*, Volume 17, Issue 1, pp. 39-58.

Soetanto, D., Lapierre, L., Pascoal, A. (2003). Adaptive, non-singular path-following control of dynamic wheeled robots. *Proceedings of the 42nd IEEE Conference on Decision and Control*, vol. 2, pp. 1765-1770.

Valenti, M., Bethke, B., Fiore, G., How, J. (2006), Indoor Multi-Vehicle Flight Testbed for Fault Detection, Isolation, and Recovery, *AIAA Guidance, Navigation, and Control Conference*, Colorado, USA.

Wang, J., Bierling, T., Höcht, L., Holzapfel, F., Klose, S., Knoll, A. (2011), Novel Dynamic Inversion Architecture Design for Quadrocopter Control, *CEAS: Conference on Guidance Navigation and Control*, München, Germany.